Thermodynamic and Conformational Characterization of 5-Methylcytosine- versus Cytosine-Substituted Oligomers in DNA Triple Helices: Ab Initio Quantum Mechanical and Free Energy Perturbation Studies

Frederick H. Hausheer,*,†,‡,⊗ U. Chandra Singh,§,⊗ Jeffrey D. Saxe,∥ John P. Flory,⊥ and Kris B. Tufto⊥

Contribution from the Molecular Design Laboratory, Cancer Therapy and Research Center, 8122 Datapoint Drive, San Antonio, Texas 78229, Division of Medical Oncology, University of Texas Health Sciences Center, San Antonio, Texas 78229, Molecular Biology, Scripps Clinic and Research Foundation, 10666 North Torrey Pines Road, La Jolla, California 92037, Sterling Research Group, 9 Great Valley Parkway, Malvern, Pennsylvania 19355, and Cray Research, Inc., 655 Lone Oak Drive, Eagan, Minnesota 55121. *Received September 13, 1991*

Abstract: Substitution of 5-methylcytosine for cytosine in DNA oligomers increases the stability of the Hoogsteen-paired third strand hybridizing to complementary double strand DNA under physiological pH conditions. The physicochemical mechanism(s) underlying the increased stability of DNA triplex formation which accompanies 5-methylcytosine substitution in the third DNA strand is poorly understood. To address these objectives, we performed ab initio quantum mechanical and statistical mechanical studies on the equilibrium geometries and solution proton affinities of 5-methylcytosine and cytosine and incorporated these into large-scale numerical simulation models of a DNA triple helical system $d[CT]_{10}$-$d[GA]_{10}$-$d[5mC+T]_{10}$. The purpose of these molecular simulations was to develop accurate models of cytosine and 5-methylcytosine nucleosides and to incorporate these structural and proton affinity models in thermodynamic and structural studies of DNA oligomer hybridization. We find that the models correctly represent the net proton affinities of cytosine and 5-methylcytosine in water and that the calculated hybridization free energy difference ($\Delta\Delta G_{hybrid}$ = 13.5 kcal/mol) between 5-methylcytosine and cytosine-substituted triple helices is qualitatively accurate. Using experimental entropy data ($\Delta S°$), we predict that 5-methylcytosine substitution into DNA oligomers stabilizes the net transition enthalpy ($\Delta H°$) of the triple helix by 73.2 kcal/mol, and a net $\Delta H°_{MEC}$ 7.3 kcal/mol per base triplet relative to the cytosine-substituted oligomer in the DNA triple helix. We observe no major conformational differences in 5-methylcytosine versus cytosine-substituted triple helices during molecular dynamics. These studies provide a greater understanding of key physicochemical mechanism(s) and properties of DNA oligomers incorporated into DNA triple helices containing 5-methylcytosine versus cytosine involved in modulating the stability of hybridization.

Introduction

Methyl substitution of the C5 atom of cytosine in DNA oligomers increases the stability of DNA triple helices at physiological pH. The mechanism(s) underlying this improved stability obtained by substituting 5-methylcytosine (MEC) for cytosine (CYT) in the third strand of the DNA triplex is poorly understood. The superior binding stability of MEC relative to CYT in triple helix formation was first described by Lee et al.[1] and has been studied more recently by other investigators.[2] These studies indicate the uniform increase in triple helix stability at neutral pH accompanying MEC relative to CYT substitution in DNA oligomers. Protonation of the N3 atom is required for CYT and MEC to form a stable DNA triple helix.[3-6] The pK_a values of CYT and MEC nucleosides are 4.3 and 4.4, respectively.[7] Thus, the relative pK_a of the nucleosides does not explain the increased stability of the triple helix which accompanies MEC incorporation into the third strand DNA oligomer binding to duplex DNA.

The generally supported structural models for DNA triple helices are based on X-ray fiber diffraction and NMR studies.[3-6,8-10] There are several physicochemical factors which influence the stability of DNA triple helix formation with regard to sequence effects, base composition, pH, cations, and other considerations.[6,10] The more commonly studied DNA triple helix systems involve an antiparallel Watson-Crick-paired polypyrimidine-polypurine system containing a collinear (parallel) Hoogsteen-paired polypyrimidine strand which is bound to the polypurine target. The conformation of pyr-pur-pyr DNA triple helices has been characterized by NMR studies[3-6] and molecular dynamics studies using explicit waters.[11] These studies demonstrate that, in the systems studied, the furanose conformations of the pyrimidine strands are C3′ endo, consistent with an A-DNA conformation, and the conformation of the furanose puckers in the purine strand are generally consistent with a B-DNA conformation.

Several groups have recently reported thermodynamic studies on DNA triple helix formation and stability in a variety of systems and under different conditions.[12-15] The major observations from these studies are that the binding affinity of the third strand is significantly lower than the binding affinity between the two Watson-Crick-paired strands and that third strand hybridization

† Cancer Therapy and Research Center.
‡ University of Texas Health Sciences Center.
§ Scripps Clinic and Research Foundation.
∥ Sterling Research Group.
⊥ Cray Research, Inc.
* Present address: BioNumerick Pharmaceuticals, 8122 Datapoint Drive, San Antonio, TX 78229.

(1) Lee, J. S.; Woodsworth, M. L.; Latimer, L. J. P.; Morgan, A. R. *Nucleic Acids Res.* **1984**, *12*, 6603-6614.
(2) Posvic, T. J.; Dervan, P. B. *J. Am. Chem. Soc.* **1989**, *111*, 3059-3061.
(3) Rajagopal, P.; Feigon, J. *Biochemistry* **1989**, *28*, 7859-7870.
(4) Rajagopal, P.; Feigon, J. *Nature* **1989**, *339*, 637-640.
(5) de los Santos, C.; Rosen, M.; Patel, D. *Biochemistry* **1989**, *28*, 7282-7289.
(6) Pilch, D. S.; Levinson, C.; Shafer, R. H. *Proc. Natl. Acad. Sci. U.S.A.* **1990**, *87*, 1947-1946.
(7) Hall, R. H. *The Modified Nucleosides in Nucleic Acids*; Columbia Univ. Press: New York, 1971; p 192-194.
(8) Felsenfeld, G.; Davies, D. R.; Rich, A. *Nature* **1957**, *79*, 2023-2024.
(9) Arnott, S.; Selsing, E. *J. Mol. Biol.* **1974**, *88*, 509-521.
(10) Kohwi, Y.; Kohwi-Shigematsu, T. *Proc. Natl. Acad. Sci. U.S.A.* **1988**, *85*, 3781-3785.
(11) Hausheer, F. H.; Singh, U. C. S.; Saxe, J. D.; Colvin, O. M.; Ts'o, P. O. P. *Anti-Cancer Drug Des.* **1990**, *5*, 159-167.
(12) Plum, G. E.; Park, Y. W.; Singleton, P. B.; Breslauer, K. J. *Proc. Natl. Acad. Sci. U.S.A.* **1990**, *87*, 9436-9440.
(13) Pilch, D. S.; Brousseau, R.; Shafer, R. H. *Nucleic Acids Res.* **1990**, *18*, 5743-5750.
(14) Manzini, G.; Xodo, L.; Gasparotto, D.; Quadrifoglio, R.; van der Marel, G. A.; van Boom, J. H. *J. Mol. Biol.* **1990**, *213*, 833-843.
(15) Xodo, L. E.; Manzini, G.; Quadrifoglio, R. *Nucleic Acids Res.* **1990**, *18*, 3557-3564.

0002-7863/92/1514-5356$03.00/0

is pH dependent when cytosine is in the oligomer. Plum et al.[12] studied cytosine versus 5-methylcytosine substitution in the third strand oligomer and observed an increase in the thermal stability, evidenced by a 10 °C increase in the Tm for the third strand at all pH values with 5-methylcytosine substitution in the oligomer. In this study, it was also observed by CD studies that there were no global structure differences between 5-methylcytosine versus cytosine-substituted triple helices.[12]

It is notable that none of these studies report thermodynamic or structural data for MEC versus CYT substitution in oligomers and the effects on triplex formation and stability.[12-15] It would be useful to understand the essential physicochemical component(s) involved in increasing triplex stability accompanying MEC substitution in oligomers, since the utility of using triplex-forming agents as diagnostic and therapeutic agents is dependent upon these properties under physiological conditions. The application of modified DNA oligomers targeted to selectively hybridize to native dsDNA has numerous potential diagnostic and therapeutic applications for modulation of DNA signal transduction events. Cytosine methylation is biologically important, playing a critical role in modulation of cellular signal transduction and regulation of transcriptional events in normal and malignant cells, and methylation of cytosine at the fifth position clearly increases the stability of duplex DNA.[16] There is increasing evidence that DNA triple helices may be biologically important, especially with the identification of several triplex-prone sequences in a variety of eukaryotic gene sequences.[17-21]

The development and application of robust molecular simulation methods have proven useful in a variety of nucleic acid systems, including DNA triple helices.[11,16,24] We have been interested in further developing and applying this methodology to determine relative Gibbs free energy binding affinities for larger molecular perturbations (e.g., up to several hundred atoms) involving DNA oligomers. There is significant research value in prospectively making qualitatively accurate determinations of the relative Gibbs free energy of target binding for two different macromolecular systems in advance of chemical synthesis and experimental physicochemical characterization. The objective of the molecular simulations reported herein was to (1) develop models capable of accurate representation of physicochemical properties on a small scale e.g., nucleosides, and (2) incorporate these models to determine the feasibility and semiquantitative accuracy of prospectively calculating hybridization free energies for macromolecular nucleic acid systems involving the chemical perturbation of several hundred atoms within a DNA oligomer binding to a dsDNA target. This approach was necessary to study the difference in Gibbs free energy of MEC- and CYT-substituted DNA oligomers binding to a duplex DNA target. In addition, the dynamic physicochemical properties of the DNA triplex and single strand MEC versus CYT-substituted oligomers were studied in an attempt to learn of the conformational properties associated with each chemical state of the DNA oligomer in the hybridized state.

Methods

Ab Initio Quantum Mechanical Studies of Nucleosides. The equilibrium geometries and partial atomic charge assignments for protonated and unprotonated 1,5-dimethylcytosine and 1-methylcytosine were calculated using ab initio quantum mechanical methods at the Hartree–Fock level using QUEST.[22] Ab initio quantum mechanical SCF gradient (geometry) optimizations were performed using an RHF 3-21G* basis set.[23] All internal degrees of molecular freedom were optimized to a convergence cutoff criterion of <0.001 Hartree/Bohr (<0.627 kcal/mol). All-atom (with explicit aliphatic hydrogens) partial atomic charges and proton affinity energies for MEC and CYT were derived from ab initio wave functions using a 6-31G* basis set.[23] The monopole atomic charges were fitted to the ab initio calculated molecular electrostatic potential.[22] The final monopole atomic charge assignments for the MEC and CYT nucleotide fragments were balanced to obtain a net charge of +1 for each protonated base, sugar, and phosphodiester unit in the DNA. The calculated charges for these nucleosides are uniformly consistent with published RHF 6-31G* fitted atomic charges for nucleic acids in the database.[24]

Free Energy Perturbation Methodology. The series of numerical expression for free energy calculations were derived from statistical mechanical perturbation theory originally proposed by Zwanzig.[25] and have been implemented into AMBER programs[26-28] to enable characterization of free energy differences for a variety of chemical and biological systems. All molecular mechanics, molecular dynamics, and free energy calculations of the nucleosides, the DNA triple helix, and the single strand DNA oligomer were made with a fully vectorized, parallel version of AMBER using an all-atom force field (version 3.2) optimized for Cray supercomputers.[27] All molecular simulations were performed on a Cray Y-MP 8/64. The single processor CPU time for the AMBER free energy perturbation of the DNA triple helix was 224 h, with an average execution speed of 114.8 MFLOPS.

For computing differences in solvation free energy, $\Delta\Delta G_{sol}$, between protonated and unprotonated states of a molecule as in the case of MEC versus CYT nucleosides, the following expression was used:[28]

$$\Delta\Delta G_{sol} = \sum_{i=0}^{N} \Delta\Delta G_i = -kT \sum_{i=0}^{N} \ln \langle \exp[-\beta(U(\lambda_{i+1}) - U(\lambda_i))] \rangle_i$$

where $\beta = 1/kT$ and $\langle\rangle_i$ describes the mean value of $\Delta\Delta G_{sol}$ calculated over the state coupled to parameter λ_i. Using this approach in combination with the coordinate coupling method (vide infra), $\Delta\Delta G_{sol}$ is calculated as a function of the presence or absence of the N3 proton on the nucleoside.

The SCF optimized equilibrium geometries and atomic point charges for the reference and perturbed chemical states were used for the free energy difference calculations by the application of the coordinate coupling method, which is represented by the following expression:

$$X_{AB\lambda} = \lambda X_A + (1 - \lambda)X_B \qquad 0 \le \lambda \le 1$$

The coordinate coupling method[26] stringently couples the transition (as a function of λ) between the two equilibrium geometries (represented as X_A and X_B). In addition, the electrostatic and van der Waals components of the initial and final chemical states are stringently coupled as a function of λ during the molecular perturbation for calculation of the free energy differences in solvation and hybridization.

Molecular Mechanics and Molecular Dynamics Simulations. Nucleoside Simulations. The ab initio quantum mechanical optimized molecular structures and energies of protonated and unprotonated MEC and CYT were used to calculate the net proton affinities in water. The differences in solvation free energy for the protonated and unprotonated states of MEC and CYT was calculated by the free energy methods described for proton affinity.[28] The nucleosides were surrounded by a 32-Å diameter sphere of TIP3P[29] waters. The systems were prepared for calculation of the solvation free energy difference as a function of the protonated and unprotonated chemical states of MEC and CYT by a series of stepwise numerical simulations. Each solvated nucleoside was prepared for free energy perturbation by sequential energy minimization of the waters alone (for 2500 cycles) and then by minimization of the waters and the nucleoside (for 2500 cycles), followed by acclimation of the system to SHAKE[30] bond constraints for 100 cycles. The bond constraints were used

(16) Hausheer, F. H.; Rao, S. N.; Gamcsik, M. P.; Kollman, P. A.; Colvin, O. M.; Saxe, J. D.; Nelkin, B. D.; McLennan, I. J.; Barnett, G.; Baylin, S. B. *Carcinogenesis* **1989**, *10*, 1131–1137.
(17) Wells, R. D.; Collier, D. A.; Hanvey, J. C.; Shimizu, M.; Wohlrab, F. *FASEB* **1988**, *2*, 2939–2949.
(18) Hanvey, J. C.; Shimizu, M.; Wells, R. D. *Proc. Natl. Acad. Sci. U.S.A.* **1988**, *85*, 6292–6296.
(19) Johnston, B. H. *Science* **1988**, *241*, 1800–1804.
(20) Mirkin, S. M.; Lyamichev. V. I.; Drushlyak, K. N.; Dobrynin, V. N.; Filippov, S. A.; Frank-Kamenetskii, M. D. *Nature* **1987**, *330*, 495–497.
(21) Lyamichev, V. I.; Mirkin, S. M.; Frank-Kammenetskii, M. D.; Cantor, C. R. *Nucleic Acids Res.* **1988**, *16*, 2165–2178.
(22) Singh, U. C.; Kollman, P. A. *J. Comput. Chem.* **1984**, *2*, 129–145.
(23) (a) 3-21G basis set: Binkley, J. S.; Pople, J. A.; Hehre, W. J. *J. Am. Chem. Soc.* **1980**, *102*, 939. (b) 6-31G* basis set: Hariharan, P. C.; Pople, J. A. *Theor. Chim. Acta* **1973**, *28*, 213.
(24) Hausheer, F. H.; Singh, U. C. S.; Palmer, T. J.; Saxe, J. D. *J. Am. Chem. Soc.* **1990**, *112*, 9468–9474.
(25) Zwanzig, R. W. *J. Chem. Phys.* **1954**, *22*, 1420–1426.
(26) Singh, U. C.; Brown, F. K.; Bash, P. A.; Kollman, P. A. *J. Am. Chem. Soc.* **1987**, *109*, 1607–1614.
(27) Singh, U. C.; Weiner, P. K.; Seibel, G.; Kollman, P. A. AMBER version 3.2, 1989.
(28) Cieplak, P.; Bash, P.; Singh, U. C.; Kollman, P. A. *J. Am. Chem. Soc.* **1987**, *109*, 6283–6289.
(29) Jorgenson, W. L.; Chandrasekkar, J.; Madura, J. D.; Impey, R. W.; Klein, M. L. *J. Chem. Phys.* **1983**, *79*, 926–935.

to enable a larger time step during molecular dynamics and free energy perturbation (0.002 ps). Molecular dynamics equilibration of the systems was carried out over 10-ps trajectories at 300 K. The equilibration of the systems was verified by acceptable values in the mean fluctuations of the system energy and temperature. The difference in solvation free energy for the protonated and unprotonated states of MEC and CYT was carried out over a 200-ps trajectory at 300 K.

Triple Helix Simulations. Cartesian molecular coordinates of d-$[CT]_{10}$-d$[GA]_{10}$-d$[5mC+T]_{10}$ were built using coordinates from DNA triple helices determined from X-ray fiber diffraction data.[9] Single strand molecular coordinates for the d$[5mC+T]_{10}$ oligomer were taken from the starting geometry for the triplex. The phosphodiester moieties of the triplex were neutralized by the placement of Mg^{2+} atoms between anionic phosphate oxygens of the second and the third DNA strands near the midpoint between the phosphate groups. Na^+ counterions were coordinated to each phosphate group in the first strand of the triple helix to maintain the electroneutrality of the system. There are 38 counterions (19 Mg^{2+} and 19 Na^+) in the triple helix system, and 19 counterions (Na^+) were coordinated to the single strand d$[5mC+T]_{10}$ system. The total number of atoms in the DNA triple helix and the single strand DNA oligomer is 1965 and 678 atoms, respectively.

The molecular mechanics, molecular dynamics, and free energy calculations of the DNA triple helix and single strand oligomer were conducted without explicit water molecules using a distance-dependent dielectric ($e = R_{ij}$) to approximate the dielectric shielding of water. Explicit waters were not included in these pilot simulations because of the significant increase in the computational complexity accompanying this large number of atoms undergoing chemical perturbation. A 12-Å nonbonded cutoff distance was used for calculation of the van der Waals and electrostatic forces, and the atom pair list for calculation of the forces was updated every 25 steps during the energy minimization, molecular dynamics, and free energy perturbation calculations. The longer cutoff distance (e.g., greater than 8–10 Å) was used because of the size of the DNA system, ~68 Å, and because of the pilot nature of these simulations. The DNA systems were energy minimized without constraints for 5000 cycles (the final rms gradients were <0.01 kcal/mol/Å), followed by 200 cycles of energy minimization with bond constraints activated.[30] Molecular dynamics at constant temperature (300 K) was carried out with SHAKE bond constraints to enable a larger time step of 0.002 ps during molecular dynamics and Gibbs free energy determinations. Prior to running the free energy perturbation trajectory, each system was equilibrated by a prior 10-ps run of molecular dynamics at 300 K. The mean temperature and total energy fluctuations were 1.6% and 2.2%, respectively, of the corresponding average total values during the last 5 ps of the initial 10-ps trajectories. The results are similar for the single strand oligomer (data not shown). There were no detectable artifacts due to inaccuracies in numerical integration in any of the simulations. Data analysis of the molecular dynamics run for the free energy perturbation of the DNA triple helix and single strand DNA oligomer was made on the initial (0–200 ps) and final (200–400 ps) perturbation dynamics trajectories generated after equilibration.

For computing differences in free energies of hybridization ($\Delta\Delta G_{hybrid}$) between the single strand oligomer and the double strand DNA target (d$[CT]_{10}$-d$[GA]_{10}$) as a function of the perturbation from d$[5mC+T]_{10}$ → d$[C+T]_{10}$, the following thermodynamic cycle is employed:

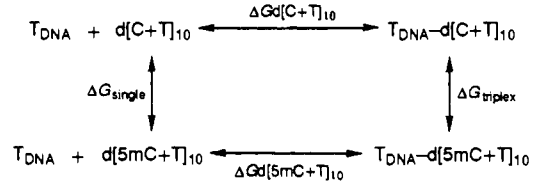

This allows determination of the difference in free energy of hybridization of the oligomer as $\Delta\Delta G_{hybrid} = \Delta G_{d[5mC+T]_{10}} - \Delta G_{d[C+T]_{10}} = \Delta G_{triplex} - \Delta G_{single}$. $\Delta G_{d[5mC+T]_{10}}$ and $\Delta G_{d[C+T]_{10}}$ are the (experimental) free energy changes for the hybridization of the strands d$[5mC+T]_{10}$ and d$[C+T]_{10}$ with the target strand T_{DNA}, respectively. ΔG_{single} and $\Delta G_{triplex}$ are the calculated free energy changes for the mutation of the strand d$[5mC+T]_{10}$ to d$[C+T]_{10}$ as a monomer in solution and as a triple-stranded DNA complex with the target double strand (T_{DNA}) in solution, respectively. The intrinsic free energy difference, $\Delta\Delta G_{single}$, as a function of the chemical perturbation within the unbound (free) single strand DNA oligomer, is expected to be close to zero. Therefore, the value of $\Delta G_{triplex}$ will be nearly the same as that calculated by $\Delta\Delta G_{hybrid}$. To be certain of this, we performed the direct calculation of ΔG_{single} for this mutation. It is important to note that the experimental data used for comparison with the calculated values for these mutations are measured Tm values. In this instance, calculations for $\Delta G_{triplex}$ and $\Delta\Delta G_{hybrid}$ for each mutation in the triple helical DNA complex in solution are an appropriate means to study these problems.

Free energy perturbation calculations of the DNA triple helix and unbound single strand oligomer were conducted as follows. The free energy difference in d$[5mC+T]_{10}$ versus d$[C+T]_{10}$ oligomers binding to a duplex DNA target and as a free single strand DNA oligomer were determined from a 400-ps molecular dynamics trajectory. The Gibbs free energy hybridization calculation involved the chemical perturbation of 10 MEC nucleoside residues (base and furanose) to 10 CYT nucleoside residues within the third strand oligomer. To correct for the intrinsic free energy differences of the two chemical states (MEC and CYT) of the single strand DNA oligomer, the net sum of the ΔG_{single} value and $\Delta G_{triplex}$ was used to calculate the corrected difference in hybridization free energy, $\Delta\Delta G_{hybrid}$. The thermodynamic and chemical coupling partition (λ) for these calculations varied between 0.0001 and 0.01, and approximately 175 incremental perturbations of λ were completed for each perturbation trajectory. Each thermodynamic partition of λ consisted of 500–1000 steps of thermal equilibration (1–2 ps), followed by 500–1000 steps of statistical data collection (1–2 ps) using a 0.002-ps time step throughout the trajectory. The temperature of the systems was maintained close to 300 K throughout by intermittent scaling of the velocities of the atoms at 0.5-ps intervals. The perturbation trajectory was calculated in the forward (MEC → CYT) and reverse (CYT → MEC) directions at each thermodynamic window $\Delta G(\lambda_i)$ to evaluate for hysteresis and numerical artifacts of the simulations.

Table I. Neutral Cytosine: Comparison of X-ray Crystal and Hartree–Fock (3-21G*) Equilibrium Geometries[a]

	X-ray crystal	calcd	expt − calcd
	Bond Lengths		
C1–N1	1.468	1.471	0.003
N1–C6	1.360	1.354	−0.006
N1–C2	1.392	1.421	0.029
C6–C5	1.357	1.340	−0.017
C5–C4	1.433	1.436	0.003
C4–N4	1.324	1.343	0.019
C4–N3	1.339	1.297	−0.042
N3–C2	1.358	1.365	0.007
C2–O2	1.237	1.215	−0.022
	absolute mean error = 0.016 Å		
	relative mean error = −0.003 Å		
	Bond Angles		
C1–N1–C6	121.5	120.9	−0.6
C1–N1–C2	118.2	118.0	−0.2
N1–C6–C5	121.2	122.2	1.0
N1–C2–N3	118.6	115.9	−2.7
N1–C2–O2	118.9	119.2	0.3
C6–C5–C4	117.0	115.9	−1.1
C6–N1–C2	121.2	121.0	−0.2
C5–C4–N4	120.1	119.8	−0.3
C5–C4–N3	121.5	122.2	0.7
C4–N3–C2	120.5	122.6	2.1
N4–C4–N3	120.1	117.9	−2.2
N3–C2–O2	122.5	124.7	2.2
	absolute mean error = 1.1 deg		
	relative mean error = −0.1 deg		

[a] Bond lengths are in angstroms, and angles are in degrees.

Results

Physicochemical Studies of MEC and CYT Nucleosides. The feasibility of using large-scale molecular dynamics and free energy perturbation simulations was validated by developing accurate small-scale simulations of individual nucleosides. To develop and refine small-scale molecular models suitable for large scale simulations, it was essential that the models accurately represent key physicochemical properties of the systems of interest. Since we were interested in studying the differences in MEC versus CYT substitution and their mechanism(s) governing the binding affinity of the oligomer, it was essential to establish that such models accurately describe the equilibrium nucleoside geometries and the net differences in proton affinity of the nucleosides in water. The ab initio quantum mechanical (RHF 3-21G*) computed equi-

(30) Van Gunstersen, W. F.; Berendsen, H. J. C. *Mol. Phys.* **1977**, *34*, 1311–1327.

Table II. Protonated Cytosine: Comparison of X-ray Crystal and Hartree–Fock (3-21G*) Equilibrium Geometries[a]

	X-ray crystal	calcd	expt − calcd
	Bond Lengths		
C1–N1	1.480	1.496	0.016
N1–C6	1.355	1.347	−0.008
N1–C2	1.395	1.385	−0.010
C6–C5	1.358	1.350	−0.008
C5–C4	1.411	1.413	0.002
C4–N4	1.319	1.313	−0.006
C4–N3	1.344	1.342	−0.002
N3–C2	1.392	1.403	0.011
C2–O2	1.204	1.198	−0.006
	absolute mean error = 0.008 Å relative mean error = −0.001 Å		
	Bond Angles		
C1–N1–C6	120.0	121.1	1.1
C1–N1–C2	117.6	117.5	−0.1
N1–C6–C5	123.1	123.7	0.6
N1–C2–N3	113.7	113.9	0.2
N1–C2–O2	124.2	124.7	0.5
C6–C5–C4	117.8	117.7	−0.1
C6–N1–C2	122.1	121.2	−0.9
C5–C4–N4	121.3	123.2	1.9
C5–C4–N3	118.4	117.2	−1.2
C4–N3–C2	125.3	125.9	0.6
N4–C4–N3	120.2	119.5	−0.7
N3–C2–O2	122.0	121.2	−0.8
	absolute mean error < 0.7 deg relative mean error < 0.1 deg		

[a] Bond lengths are in angstroms, and angles are in degrees.

Table III. Neutral and Protonated 5-Methylcytosine: Hartree–Fock (3-21G*) Equilibrium Geometries[a]

	neutral	protonated	prot − neut
	Bond Lengths		
C1–N1	1.469	1.493	0.024
N1–C6	1.357	1.349	−0.008
N1–C2	1.414	1.378	−0.036
C6–C5	1.342	1.353	0.011
C5–C4	1.447	1.421	−0.026
C4–N4	1.345	1.316	−0.029
C4–N3	1.298	1.345	0.047
N3–C2	1.362	1.400	0.038
C2–O2	1.216	1.200	0.016
C7–C5	1.518	1.520	0.002
	Bond Angles		
C1–N1–C6	120.6	120.8	0.2
C1–N1–C2	118.4	118.0	−0.4
N1–C6–C5	123.5	125.2	1.7
N1–C2–N3	115.4	113.4	−2.0
N1–C2–O2	119.6	125.2	5.6
C6–C5–C4	114.1	115.8	1.7
C6–N1–C2	120.9	121.1	0.2
C5–C4–N4	121.0	124.2	3.2
C5–C4–N3	122.5	117.6	−4.9
C4–N3–C2	123.3	126.6	3.3
N4–C4–N3	116.3	118.1	1.8
N3–C2–O2	124.9	121.3	−3.6
C7–C5–C6	121.6	120.1	−1.5
C7–C5–C4	124.2	123.9	−0.3

[a] Bond lengths are in angstroms, and angles are in degrees.

librium bond lengths and angles for protonated and unprotonated species of CYT and MEC are shown in Tables I–III. The calculated equilibrium geometries are in reasonable agreement with X-ray crystallographic data (R = 0.085–0.115)[31] for unprotonated and protonated CYT. The absolute mean error in geometries is greater for the unprotonated than for the protonated CYT species. In general, the calculated bond lengths are somewhat shorter than these in the X-ray structures. The performance of the theory in terms of characterizing the structural features of these molecules is in keeping with the benchmarking and calibration work of Lothar Schafer et al.[32] The SCF calculated (RHF 6-31G*) atomic point charges fitted to the molecular electrostatic potential for CYT and MEC are shown in Figure 1.

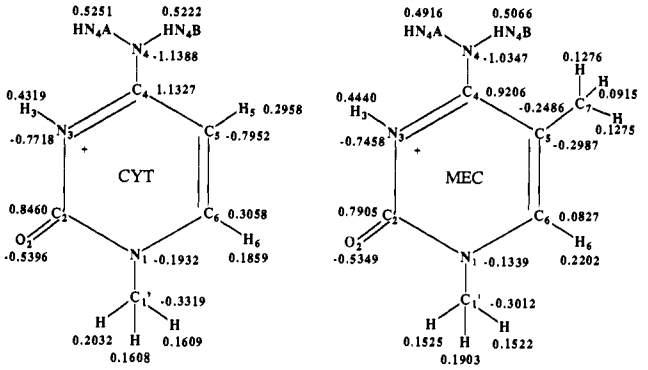

Figure 1. Ab initio quantum mechanical (RHF 6-31G*) ESP charges for N3-protonated cytosine (CYT) and N3-protonated 5-methylcytosine (MEC).

Table IV. Calculated Net Proton Affinities for N1-Methylcytosine and N1,C5-Methylcytosine

gas-phase enthalpies (hartrees)	cytosine	5-methylcytosine
unprotonated	−431.642848	−470.674534
protonated	−432.036179	−471.071132
proton affinity	−0.393331	−0.396597
proton affinity (kcal)	−246.8	−248.8
$\Delta\Delta G_{sol}$ [hysteresis] (kcal)	−32.8 [0.3]	−30.8 [0.2]
net proton affinity in water	−279.6	−279.6
experimental pK_a[7]	4.4	4.3

Table V. Free Energy Differences between d[5mC+T]$_{10}$ and d[C+T]$_{10}$ Hybridization within the DNA Triple Helix and as a Single Strand Oligomer at 300 K

	ΔG MEC+ → CYT+	ΔG CYT+ → MEC+	hysteresis
$\Delta G_{triplex}$	15.3	−13.7	0.8
ΔG_{single}	−0.8	1.1	0.1
$\Delta\Delta G_{hybrid}$	14.5	−12.6	1.9

Calculation of the net proton affinities for MEC and CYT nucleosides in water at 300 K was made by combined use of the gas-phase affinities and the solvation free energy differences between the protonated and unprotonated species of MEC and CYT. The data from these numerical simulations are given in Table IV. The calculated net proton affinities in water for MEC and CYT are identical, an observation that is in excellent agreement with the experimental pK_a values of the nucleosides.[7] These data document the accuracy of the small-scale nucleoside models in reproducing the proton affinities of MEC and CYT in water since the experimental difference in pK_a is 0.1 pH unit. The gas-phase proton affinity of MEC is 2.0 kcal/mol greater than that of CYT, and in solution this value is diametrically offset by a 2.0 kcal/mol reduction from solvation effects. The C5 methyl group of MEC is the major factor which reduces the solvation free energy and is most likely due to hydrophobic interactions with water. After validation of the performance of the models on a small scale, large-scale simulations on the DNA triple helix were carried out.

Thermodynamic Studies of the DNA Triple Helix. The calculated Gibbs free energy difference ($\Delta\Delta G_{hybrid}$) in hybridization between d[5mC+T]$_{10}$ and d[C+T]$_{10}$ substituted oligomers to the target d[CT]$_{10}$-d[GA]$_{10}$ is shown in Table V. The free energy

(31) Voet, D.; Rich, A. *Prog. Nucleic Acid Res. Mol. Biol.* **1970**, *10*, 183–265.

(32) Schafer, L.; Ewbank, J. D.; Klimkowski, V. J.; Siam, K.; Alsenoy, C. V. *J. Mol. Struct.* **1986**, *135*, 141–158.

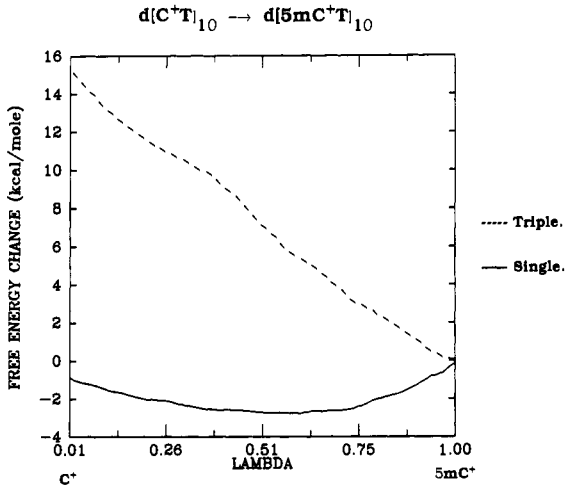

Figure 2. Free energy perturbation profile of $d[C+T]_{10} \rightarrow d[5mC+T]_{10}$ within the DNA triple helix (---) and as the unbound single strand oligomer (—) at 300 K.

Table VI. Thermodynamic Statistics during Free Energy Perturbation and Molecular Dynamics Trajectories for d[CT]-d[GA]-d[5mC+T] and d[C+T]

	triple helix	single strand
total atoms	1965	678
perturbed atoms	310	310
average temperature (rms)	299.8 K (±2.7)	299.8 K (±4.7)
average total energy (rms)	−7349.1 (±8.6)	−1695.2 (±4.8)
mean temperature fluctuation (%)	0.9	1.5
mean total energy fluctuation (%)	0.1	0.3

profiles of the unbound single strand oligomer and the triple helix are shown in Figure 2. The corrected net difference in Gibbs free energy ($\Delta\Delta G_{hybrid}$) favors MEC substitution over CYT in the DNA oligomer binding to the duplex DNA target by 13.5 kcal/mol. Using the general thermodynamic equation $\Delta G° = \Delta H° - T\Delta S°$, where $\Delta\Delta G_{hybrid}$ represents the incremental difference between $\Delta G°_{CYT}$ and $\Delta G°_{MEC}$, we can use the calculated incremental value for $\Delta G°_{MEC}$ (13.5 kcal/mol) with the experimentally determined $\Delta S°$ value of 97.6 (±7) cal/mol·K[12] for a cytosine-substituted polypyrimidine oligomer to predict the net value and incremental change in the transition enthalpy, $\Delta H°_{MEC}$. Using the experimental data[12] for $\Delta H°_{CYT}$ (30.4 ± 0.2 kcal/mol) in combination with our calculated incremental difference in $\Delta H°_{MEC}$ allows us to estimate the absolute value of $\Delta H°_{MEC}$ in MEC-substituted oligomers. Using this combined approach, our predicted differential increase in $\Delta H°_{MEC}$ relative to $\Delta H°_{CYT}$ is 42.8 kcal/mol, and the absolute net value of $\Delta H°_{MEC}$ is 73.2 kcal/mol. On the basis of these data, a net $\Delta H°_{MEC}$ of 7.3 kcal/mol and an incremental increase in the transition enthalpy of 4.3 kcal/mol per base triplet favoring the MEC substitution over CYT in the oligomer for the transition from triplex to duplex are predicted. The calculated $\Delta\Delta G_{hybrid}$ value corresponds to an equilibrium constant (K_{eq}) for the MEC-substituted oligomer of 6.8×10^9, which supports the conclusion that under equilibrium conditions the great majority of MEC-substituted oligomers are hybridized to the DNA target relative to hybridized CYT-substituted oligomers. In calculating values for $\Delta\Delta G_{hybrid}$, $\Delta H°_{MEC}$, and K_{eq}, we are assuming negligible differences in the absolute value of $\Delta S°$ for MEC and CYT oligomers and various thermodynamic properties, such as the heat capacity of the initial and final states under experimental conditions.

The average equilibrium thermodynamic behavior of the free energy molecular dynamics trajectories for the DNA triple helix and single strand oligomer are summarized in Table VI. It is notable that the forward and reverse calculations of $\Delta G_{triplex}$ and ΔG_{single} have statistical fluctuations in energy of less than 1 kcal/mol in either direction of the perturbation trajectory (Table V). Maintenance of near-equilibrium conditions during each

Table VII. Mean Hydrogen Bond Distances (rms) from Molecular Dynamics Trajectory[a]

bond	d[5mC+T]10	d[C+T]10
Watson–Crick		
THY H3–ADE N1	2.23 (0.22)	2.17 (0.09)
THY O4–ADE HN6B	1.91 (0.12)	1.90 (0.09)
CYT N3–GUA H1	1.97 (0.16)	1.96 (0.10)
CYT HN4B–GUA O6	2.28 (0.29)	2.31 (0.20)
CYT O2–GUA HN2A	2.01 (0.19)	2.01 (0.01)
Hoogsteen		
GUA N7–CYT H3	2.58 (0.27)	2.52 (0.11)
GUA O6–CYT HN4A	2.52 (0.21)	2.43 (0.18)
ADE N7–THY H3	2.95 (0.23)	2.48 (0.12)
ADE HN6A–THY O4	1.97 (0.29)	1.87 (0.07)

[a] Bond distances are measured in angstroms.

Table VIII. Average Helical Repeat Angles from Molecular Dynamics Trajectory[a]

d[5mC+T]10	d[C+T]10
33.5 (2.9)	32.6 (1.5)

[a] Angles are in degrees.

Table IX. Mean Base Height Distances during Molecular Dynamics[a]

strand	d[5mC+T]10	d[C+T]10
1	3.14 (0.08)	3.21 (0.08)
2	3.11 (0.07)	3.20 (0.08)
3	3.27 (0.08)	3.40 (0.09)

[a] Distances are in angstroms.

perturbation partition of λ is critical toward improving the qualitative value of determining the hybridization free energy for these large molecular perturbations. Since these calculations involved the chemical perturbation of 310 atoms in the chemical transformation within the entire DNA oligomer from MEC to CYT, it was essential to carefully monitor the thermodynamic equilibration of the system at each coupling partition of λ. This was done to ensure that no large energetic or temperature fluctuations occurred during the transition of λ in the chemical perturbation from MEC to CYT in the oligomer.

Molecular Dynamics Studies of the DNA Triple Helix. The molecular dynamics trajectory during MEC to CYT perturbation in the oligomer was studied to characterize various conformational properties as a function of MEC versus CYT substitution within the DNA oligomer hybridized to form the triple helix. To accomplish this analysis, an analysis of the time-averaged molecular dynamics trajectory of the triple helix was analyzed as a function of the chemical state of the third strand with respect to MEC versus CYT substitution in the oligomer. The chemical state of the DNA oligomer within the triplex is simply defined as predominantly MEC at values of $\lambda = 1.0 \rightarrow 0.5$ and CYT at values of $\lambda = 0.5 \rightarrow 0.0$. The time-averaged coordinates from each chemical state of the molecular dynamics trajectory were studied using these definitions.

The time-averaged hydrogen bond lengths are similar for MEC- and CYT-substituted oligomers within the DNA triple helical complex during molecular dynamics (Table VII). In general, the Watson–Crick and Hoogsteen hydrogen bond pairs are only slightly foreshortened and have smaller fluctuations in position in the CYT-substituted oligomer. The hydrogen bonds of the Watson–Crick- and Hoogsteen-paired bases remained intact throughout the simulation in both triple helix DNA systems.

The time-averaged mean helical repeat angles of the dsDNA portion of the triple helix differ by 0.9 degrees (Table VIII) as a function of methyl substitution of cytosine. This difference in the mean helical repeat angle indicates that the MEC duplex has slightly fewer base pairs than CYT (10.7 versus 11.0 base pairs) per helical turn in the duplex portion of the triplex. This slight unwinding of the dsDNA helix in the case of MEC relative to CYT is plausible, since the CYT oligomer has less steric bulk in the major groove due to the absence of the C5 methyl group. The

Table X. Furanose Populations (%) from Molecular Dynamics Trajectory

	C3′-endo		O1′-endo		C2′-endo		other	
	5mC+	C+	5mC+	C+	5mC+	C+	5mC+	C+
$d[CT]_{10}$	93	94	5	0	4	5	1	1
$d[GA]_{10}$	81	77	5	3	10	14	5	6
$d[mC+T]_{10}$	34	31	13	16	51	52	2	0

Table XI. Mean Intrastrand (A) and Interstrand (B) Phosphorus Atom Distances from Molecular Dynamics Trajectory[a]

	$d[5mC+T]_{10}$	$d[C+T]_{10}$
	A. Intrastrand	
$d[CT]_{10}$	5.8 (0.2)	5.8 (0.0)
d[GA]	6.2 (0.1)	6.2 (0.1)
$d[5mCT]_{10}$	6.7 (0.1)	6.7 (0.1)
	B. Interstrand	
1–2	16.9 (0.3)	16.9 (0.2)
2–3	9.6 (0.2)	9.5 (0.1)
1–3	19.2 (0.4)	19.2 (0.2)

[a] Distances are in angstroms.

base height distance in the CYT triplex is consistently increased in contrast to the MEC-substituted triple helix, as shown in Table IX. The helical repeat angles and base height values are consistent with an A-DNA conformation of the duplex DNA portion of the triple helix for both substitutions.

Analysis of furanose conformational subpopulations as a function of MEC versus CYT substitution in the DNA triple helix, shown as percentages of the total population for the entire trajectory is given in Table X. These data indicate that (1) the DNA triple helix exhibits dynamic, polymorphic conformational behavior due to the presence of multiple furanose conformational populations and (2) the predominant sugar population in each strand of the triplex is C3′ endo, consistent with an A-DNA conformation accompanying MEC versus CYT substitution. There are no major differences observed in the furanose populations as a function of MEC versus CYT substitution in the third strand nor between pyrimidine and purine furanose conformations in the first and second Watson–Crick-paired stands of the duplex (data not shown).

The average intrastrand and interstrand phosphorous atom distances are shown in Table XI. The mean interstrand and intrastrand phosphorous atom distances are similar for MEC- and CYT-substituted DNA oligomers. The lack of significant displacement of the mean positions of the phosphorous atoms as a function of MEC versus CYT is notable in particular since apparently the change in helical twist of the duplex is the primary conformational change to accompany MEC substitution in the oligomer. Apparently the steric bulk of the C5 methyl group in MEC is compensated by the slight unwinding of the duplex DNA target. The third strand remains in close approximation in the triple helical complex to hydrogen bond to the complementary DNA target by this mechanism. The intrastrand phosphorous atom distances are consistent with values observed in A-DNA type structures.[33] The mean coordination distances of Na^+ and Mg^{2+} to phosphorous atoms are shown in Table XII. The Mg^{2+} counterion is more closely associated with the second DNA strand by approximately 0.2 Å on average than with the third strand in the triplex.

Discussion

We observe from these molecular simulations that it is possible to characterize key physicochemical properties of a triple helical DNA system by numerical simulation methods at the microscopic and macroscopic levels. The combinatorial application of experimental entropy ($\Delta S°$) data with calculated $\Delta G°_{MEC}$ values enables prediction of the incremental and net values for $\Delta H°_{MEC}$ in MEC-substituted DNA oligomers hybridized within a DNA triple helical complex. On the basis of our triple helix simulation models, we do not observe large conformational differences in the DNA triple helix between MEC- and CYT-substituted oligomers in the case of $d[CT]_{10}$-d[GA]$_{10}$-$d[5mC+T]_{10}$. The only notable structural difference accompanying MEC substitution involves the slight unwinding of the dsDNA target to accommodate the bulkier C5 methyl group in the major groove and maintenance of Hoogsteen binding between the third and second strands of the triplex. The general application of molecular simulation methods, as described in this work, can be applied to provide useful information regarding the mechanism(s) which may explain some of the critical differences in thermodynamic properties as a function of chemical state in a variety of systems involving DNA and RNA.

Table XII. Mean Counterion–Phosphorus Coordination Distances[a]

	$d[5mC+T]_{10}$	$d[C+T]_{10}$
strand 1–Na^+	3.2 (0.1)	3.2 (0.1)
strand 2–Mg^{2+}	2.8 (0.1)	2.8 (0.1)
strand 3–Mg^{2+}	3.0 (0.1)	3.1 (0.1)

[a] Distances are in angstroms.

The thermodynamic and conformational data from our numerical simulations of DNA triple helices compare well to recently published experimental data from several laboratories.[12-15] Careful study of these data reveals some variations in the quantitative assessments of the thermodynamic properties of triplex formation and stability which can be attributed to differences in experimental methods and DNA systems under study. The major observations from these studies are clearly consistent with regard to the following: (1) the weaker binding affinity of the third strand, (2) the pH dependence of CYT and MEC substitution for hemiprotonation at N3, (3) the greater thermal stability of MEC over CYT substitution in the DNA triplex, and (4) the much greater enthalpy of duplex DNA complexes than that of triplex DNA complexes.[12-15] In calculating thermodynamic properties for MEC-substituted DNA triplexes, we have used the experimental value for $\Delta S°$ from Plum et al.[12] on the basis of the greater similarity of their DNA triplex system (d-[TTTTTCTCTCTCTC]) to the system we have studied here, in reference to using $\Delta S°$ values reported in other studies. In doing this, it is important to note that comparison of $\Delta S°$ from Plum et al.[12] and Pilch et al.[13] reveals only a minor difference in the absolute experimental values for $\Delta S°$ of 97.6 ± 7 cal/mol·K and 90 ± 5 cal/mol·K, respectively.

It is important to recognize that the molecular models developed for the present simulations contain carefully optimized molecular structural parameters and atomic charge assignments derived from ab initio quantum mechanical wave functions. To validate the model parameters on a small scale, these molecular models were carefully developed to accurately characterize equilibrium nucleoside geometries and proton affinities in water. The performance of the nucleoside models is reasonable and gives results which are consistent with experimental data. The large-scale simulations of the DNA triple helix are free of numerical artifacts and appear to be in reasonable accord with available experimental data. Our predicted values for $\Delta H°_{MEC}$ can be validated by experiment. We believe that the observations presented above can be extended to studies that explain the role of solvation effects which may be involved in the improved thermodynamic properties of MEC-substituted oligomers in the triplex at neutral pH. To accomplish this, it will be important to complete our ongoing efforts in large-scale simulations of DNA triple helices using explicit waters in the system. The size of a fully solvated DNA triple helical complex of 20-mer strands is approximately 90 Å in diameter and comprises more than 37 000 atoms. We believe that these significant increases in computational complexity are not justified without careful pilot simulations as described here because of the extreme computational requirements with the larger systems. We are presently attempting to study the role of solvation of the C5 methyl group in MEC in these systems, in the context of hydrophobic hydration at this site, which may partially explain improved thermal stability in MEC-substituted oligomers in-

(33) Saenger, W. *Principles of Nucleic Acid Structure*; Springer-Verlag: New York, 1984.

corporated into DNA triple helices.

The electronic and conformational properties of MEC versus CYT at the isolated nucleoside level deserve careful consideration since both protonated species are cationic and differ only by the presence or absence of a methyl group at C5. In previous studies, it has been demonstrated that the methyl group at C5 improved the binding of MEC relative to CYT when incorporated into DNA duplex systems because of increased base stacking energy.[16] This increased base stacking energy which accompanies cytosine methylation results in an improved enthalpy, $\Delta H°$, in duplex DNA and may underlie the improved stability of MEC-substituted triplex DNA complexes. It is reasonable to consider that altered intramolecular and intermolecular dielectric shielding of the positive charge of the proton at N3 may be an important feature of MEC substitution in DNA triple helices. An alteration in dielectric shielding induced by the C5 methyl group may result in a more favorable charge polarization of the MEC molecule to facilitate either Hoogsteen pairing or base stacking within the DNA triplex. We have previously noted significant changes in charge density in the region of the C5 methyl group in MEC relative to the hydrogen atom at C5 in CYT.[16] We are presently investigating whether there are any significant differences in the electronic factors between CYT and MEC which may help to develop a clear explanation of the improved thermal stability of MEC-substituted oligomers in DNA triple helices.

The utility of applying ab initio quantum mechanics and statistical mechanical methods in the study of microscopic and macroscopic properties of nucleic acid systems appears to have some utility for future research. The combined application of experimental data with numerical simulation permits semiquantitative and, in some instances, quantitative predictions which can be tested and further refined by experiment. The combined use of experimental and theoretical data, as in the present work, improves the ability to characterize key molecular mechanisms of interest in a useful and complementary manner. This integrated approach makes it possible to develop and refine hypotheses which can be tested in the laboratory. It should be clear from this work that laboratory data are essential to develop, calibrate, validate, and improve numerical models in a recursive, stepwise manner. The key role of numerical simulations will be to provide observations which should be useful in experimental design and productivity by proposing increasingly accurate estimations of physicochemical properties with reasonable confidence.

Acknowledgment. All calculations were carried out on a GRAY Y-MP 8/64 in Eagan, MN. This research was supported by academic grants from Cray Research (K-GAHM-XX-531-2-99 and K-531-1-99) and from Sterling Drug Inc.

Fulvenones and Isoelectronic Diazocyclopolyenes: Theoretical Studies of Structures and Stabilization

Michael A. McAllister and Thomas T. Tidwell*

Contribution from the Department of Chemistry, University of Toronto, Toronto, Ontario, Canada M5S 1A1. *Received November 14, 1991*

Abstract: Isodesmic energy comparisons of 6-31G*//6-31G* calculations for the fulvenes **1–3** and fulvenones **4–6** show significant destabilization for triafulvenone (**4**, −17.1 kcal) and heptafulvenone (**6**, −5.1 kcal/mol) and stabilization for pentafulvenone (**5**, 4.1 kcal/mol). These effects are attributed to enhanced antiaromatic destabilization in **4** and **6** compared to the corresponding fulvenes and enhanced aromatic stabilization in pentafulvenone (**5**) compared to pentafulvene (**2**). Analysis of dipole moments, atomic charges, and bond lengths provides further evidence for these aromaticity effects. Similar evidence is found for antiaromatic destabilization upon fluorine substitution in the exocyclic methylene group of triafulvene. Diazocyclopropene (**7**), diazocyclopentadiene (**8**), and diazocycloheptatriene (**9**) are isoelectronic with the corresponding fulvenones **4–6**, respectively, and show the corresponding destabilization and stabilization effects.

The fulvenes, especially triafulvene (**1**), pentafulvene (**2**), and heptafulvene (**3**), have attracted intense interest because of their unique conjugated structures.[1a-h] The question of the aromatic/antiaromatic character of these and similar rings has attracted particular attention.[1]

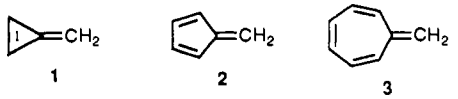

1 **2** **3**

The corresponding ketenes **4–6** may be referred to as fulvenones, with specific names of triafulvenone (**4**), pentafulvenone (**5**), and heptafulvenone (**6**).[2] Of these, **5**[3-5] and **6**[6] have been studied

(1) (a) Neuenschwander, N. Fulvenes. In *The Chemistry of Functional Groups. Supplement A. The Chemistry of Double-bonded Functional Groups.* Patai, S., Ed.; Wiley, New York, 1989; Vol. 2, Parts 1 and 2. (b) Yates, P. *Adv. Alicycl. Chem.* **1968**, *2*, 59–184. (c) Becker, G. Triafulvenes. *Houben-Weyl, Method. Org. Chem.* **1985**, *5/2c*, 476–478. (d) Zeller, K. P. Pentafulvenes. *Ibid.* **1985**, *5/2c*, 504–684. (e) Asao, T.; Oda, M. Heptafulvenes. *Ibid.* **1985**, *5/2c*, 768–780. (f) Bergmann, E. D. *Chem. Rev.* **1968**, *68*, 41–84. (g) Bachrach, S. M.; Liu, M. *J. Phys. Org. Chem.* **1991**, *4*, 242–250. (h) Jug, K.; Koster, A. M. *J. Phys. Org. Chem.* **1991**, *4*, 163–169. (i) Byun, Y.; Saebo, S.; Pittman, C. U., Jr. *J. Am. Chem. Soc.* **1991**, *113*, 3689–3696.

(2) Alternative names are cyclopropylideneketene (**4**), cyclopentylidieneketene (**5**), and cycloheptylideneketene (**6**). Chemical Abstracts names are methanone, 2-cyclopropen-1-ylidone (**4**); methanone, 2,4-cyclopentadien-1-ylidone (**5**), and methanone, 2,4,6-cycloheptatrien-1-ylidone (**6**).

(3) (a) Süs, O. *Liebigs Ann. Chem.* **1944**, *556*, 65–85. (b) Urwyler, B.; Wirz, J. *Angew. Chem., Int. Ed. Engl.* **1990**, *29*, 790–791. (c) Mamer, O. A.; Rutherford, K. G.; Seidewand, R. J. *Can. J. Chem.* **1974**, *52*, 1983–1987. (d) Bloch, R. *Tetrahedron Lett.* **1978**, 1071–1072. (e) Schulz, R.; Schweig, A. *Ibid.* **1979**, 59–62. (f) Schweig, A.; Zittlau, W. *Chem. Phys.* **1986**, *103*, 375–382. (g) Schulz, R.; Schweig, A. *Angew. Chem., Int. Ed. Engl.* **1984**, *23*, 509–511. (h) Baird, M. S.; Dunkin, I. R.; Hacker, N.; Poliakoff, M.; Turner, J. J. *J. Am. Chem. Soc.* **1981**, *103*, 5190–5195. (i) Chapman, O. L. *Pure Appl. Chem.* **1979**, *51*, 331–339. (j) Clinging, R.; Dean, F. M.; Mitchell, G. H. *Tetrahedron* **1974**, *30*, 4065–4067. (k) Tanigaki, K.; Ebbesen, T. W. *J. Phys. Chem.* **1989**, *93*, 4531–4536.

(4) (a) Thompson, L. F.; Willson, C. G.; Bowden, M. J. S. *Introduction to Microlithography*; American Chemical Society: Washington, DC, 1989. (b) De Forest, W. S. *Photoresist: Materials and Processes*; McGraw-Hill: New York, 1975; pp 132–162.

0002-7863/92/1514-5362$03.00/0